A MATHEMATICAL MODEL OF SEMICONDUCTOR DETECTOR GAMMA-EFFICIENCY CALIBRATION FOR RECTANGULAR CUBOID (BRICK-SHAPE) SOURCES

by

Nikola N. MIHALJEVIC [1,2], Slobodan I. JOVANOVIC [2,3*], Aleksandar D. DLABAC [2], and Mohamed S. BADAWI [4,5]

[1] Department of Mathematics, Maritime Faculty, University of Montenegro, Kotor, Montenegro
[2] Centre for Nuclear Competence and Knowledge Management, University of Montenegro, Podgorica, Montenegro
[3] Department of Physics, Faculty of Mathematics and Natural Sciences, University of Montenegro, Podgorica, Montenegro
[4] Department of Physics, Faculty of Science, Beirut Arab University, Beirut, Lebanon
[5] Physics Department, Faculty of Science, Alexandria University, Alexandria, Egypt

Scientific paper
http://doi.org/10.2298/NTRP1802139M

Rectangular cuboid (rectangular parallelepiped), *i. e.*, brick-shape sources are not really common in general gamma-spectrometry practice with semiconductor detectors, where axially symmetrical sources prevail. However, in some particular applications, like radioactivity control of food or construction materials (for monitoring and regulatory purposes, radiological emergency preparedness, or in the aftermath of nuclear accidents), brick shapes may come to significance. In order to simplify routine/repetitive low activity measurements, it is easier and more practical to measure the radioactivity of these sources as such, *i. e.*, without transforming them into "regular" (cylindrical or Marinelli) shapes. This saves considerably on laboratory time, workforce and consumables – thus eventually cutting the cost of analysis and improving laboratory performance. In addition, the accuracy of the analytical results is enhanced, as the possibilities for systematic errors are reduced. To that aim, in the present work a mathematical model for brick-source efficiency calibration is developed. The well known, accurate and widely used efficiency transfer principle is applied, together with detector efficiency calculations based on the effective solid angle $\overline{\Omega}$ concept. For testing purposes, comparisons are made with previously developed and well established mathematical models for detector calibration involving axially symmetrical sources (point, disc, and cylinder). Namely, brick sources were regarded as a sort of interpolation between the outer and inner cylinder of the same height, for which efficiencies could be accurately determined by numerical calculations (software ANGLE). For the sake of completeness, the *equivoluminous* cylinders were taken into account as well. Brick shape sources of various sizes and proportions were examined; when approaching zero dimensions, results were obtained for point and disc sources. All calculations were performed in gamma energy range 50-3000 keV. The results are consistent and logical, with no discrepancies indicating bugs or systematic errors – thus convincingly confirming the fundamentality and reliability of the model. The model is about to be incorporated into ANGLE software as a new functionality, so as to make it available to gamma spectrometry community.

Key words: gamma spectrometry, detection efficiency, detector calibration, rectangular cuboid source, mathematical model, numerical testing, applicability

INTRODUCTION

The need for mathematical modelling of rectangular cuboid (rectangular parallelepiped), *i. e.*, brick-shape sources in quantitative gamma spectrometry with semiconductor detectors was recognized from the beginnings of the method in 1970s, at least as a theoretical issue. However, the complexity of calculations and poor computation capabilities at the time (from one side), combined with little need/opportunities for practical application (from the other), turned out not to be a great incentive for progressing in the matter. In a number of papers, notably those from Alexandria University group [1-5], approximate or even exact analytical solutions were offered, however with more or less limited applicability. The limitations mainly concerned the source size and the details of detector depiction. For instance, in the pioneering model of Nafee and Abbas [1], a brick's vertical projection on the detector crystal should (predominantly) lie within the crystal top surface, as gamma rays entering the crystal

* Corresponding author; e-mail: bobo_jovanovic@yahoo.co.uk

through its side surface are not accounted for. Practically, this means that the sources should not be exceeding a few centiliter volumes. Gouda *et al.* [2] consider the source slabs of larger volumes, including remarkable experimental verification for up to 200 ml source volumes. Their approach is based on a very elaborate mathematical processing of three key components when calculating efficiencies, separately: the geometrical, the attenuation and the detection (in the detector crystal). The detector description is somewhat simplified. An objection to this approach – as Moens *et al.* showed [6-8] – is likely in the range of its applicability: only simultaneous (thus *not separate*) differential treatment of these three parameters enables unlimited applicability of an efficiency calculation model – in respect to source dimensions, matrix materials and counting geometries. El Khatib *et al.* [3] and Badawi *et al.* [4, 5] gave perhaps the most advanced theoretical perspective so far, based on the concept of the effective solid angle – however, limiting themselves to the scintillation NaI(Tl) detectors only; note that from the mathematical modeling standpoint, scintillation detectors exhibit far less complex construction/structure than the semiconductor ones [9].

A limitation in size is a very serious drawback when low activity sources (typically food, environmental samples, or construction materials) – with volumes ranging in liters – are counted. Moreover, these are the most likely ones to be encountered in practice. As is known in gamma spectrometry, for small samples with low activity, very long counting times have to be employed in order to collect a statistically meaningful number of counts in full-energy gamma-line peaks (FEP or ε_p). This is not only a waste of laboratory time, but also leads to degradation in the (statistical) quality of primary analytical information (gamma spectrum), because of the excessive background accumulation in the spectrum. Very long counting times should thus be avoided, in principle, whenever possible.

Another limitation concerns (over)simplifications in the detector mathematical depiction/description. Semiconductor gamma detectors are very complex in structure, with many engineering details/particularities. A mathematical description/modelling of the detector, hence, inevitably involves simplifications, the impact of which is commonly not studied/known in much detail. For instance, crystal edge rounding (bulletization) is not taken into account in any of the reported modellings. Neglecting the bulletization in efficiency calculations may lead to considerable, even dramatic systematic errors [10]. In this work, the bulletization is paid due respect and dully accounted for.

Hereby, we elaborate a generalized mathematical model of semiconductor detector calibration for the brick-shape source, one of its sides being plan-parallel with the detector top surface, while its centre is positioned either on or off the detector axis (fig. 5). The latter case (off-axis shift) is of practical significance when the detector crystal is axially displaced within its encapsulation (detector *end-cap*), which happens occasionally during detector manufacturing, transportation or just exploitation/ageing [11]. The crystal shift (which often comes with the tilt – angular displacement) can be well observed and estimated/measured on the detector radiography, but also by simple experimental procedures. In addition, many other particular details in the detector construction – like the presence of the end-cap window of any material/size, protective coatings or shields inside or outside the end-cap, the already mentioned crystal bulletization (both edge and cavity), dead-layer variations between the crystal top and side wall, *etc.* – are duly taken into account.

The model implies no limitation in source dimensions, proportions or material/matrix composition, thus making it suitable for practical/routine/repetitive low activity measurements. Large sources are recommended for the use in order to reduce counting times and background component in the spectrum. Samples can thus be measured in their original packaging (which is also accounted for in calculations, as *coatings* of the sample containers), thus eliminating the need for transforming/transferring them into other (more common) shapes, like cylindrical or Marinelli beakers (*as-it-comes* samples). This saves time, consumables and workforce, while reducing both statistical uncertainty and potential for systematic errors. It is altogether a contribution to the better performance of the laboratory – producing more results, with better accuracy, and at a lower cost.

The model – brick source functionality – is currently being incorporated into ANGLE software for semiconductor detector efficiency calculations [12]; it will be available in one of the subsequent software upgrades.

THEORETICAL

The concept of the effective solid angle ($\overline{\Omega}$) for the calculation of full-energy peak detection efficiency (ε_p) has been elaborated in detail elsewhere [6, 8, 10]. Since its introduction, by the early eighties, it has been widely accepted and successfully applied in numerous dedicated models of gamma-efficiency calculations.

Given gamma source (S) and a semiconductor detector (D) (fig. 1), the effective solid angle is defined as

$$\overline{\Omega} \qquad \underset{V_S,\, S_D}{} d\overline{\Omega} \tag{1}$$

with V_S is the source volume, S_D – detector surface exposed to the source ("visible" by the source), whereby

$$d\overline{\Omega} \quad \frac{F_{att} F_{eff}\ \mathrm{TP}\,\vec{n}_u}{\left|\mathrm{TP}\right|^3} d\sigma \tag{2}$$

is the infinitesimal effective solid angle corresponding to detector surface $d\sigma$. Here T is the point varying over V_S, P – the point varying over S_D, and $\vec{n}_u$ – the external

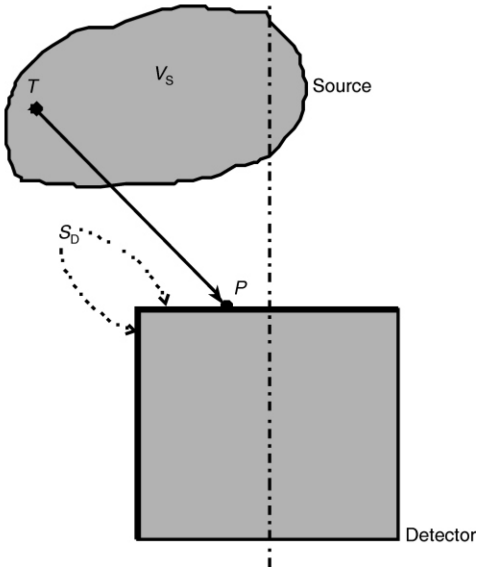

Figure 1. To the definition of the effective solid angle ($\vec{\Omega}$), eq. (1); source, detector, and their positioning are illustrated, emphasizing detector surface S_D "visible" by the source

unit vector normal to the infinitesimal area dσ at S_D. Equation (1) is thus a five-fold integral. Factor F_{att} accounts for gamma attenuation of the photon following the direction TP out of the detector active zone, while F_{eff} describes the probability of an energy degradable photon interaction with the active detector body (*i. e.* coherent scattering excluded), initiating the detector response. The two factors include, therefore, geometrical and composition-related parameters of the materials traversed by the photon.

ε_p is subsequently found as

$$\varepsilon_p \quad \frac{P}{T}\,\overline{\Omega} \tag{3}$$

where P/T is *virtual* peak-to-total ratio (*virtual* meaning it is valid for a bare isolated detector crystal in a vacuum) [6]. Fairly assuming that P/T is an intrinsic characteristic of the detector crystal (depending on gamma energy only) [13-15], implies that ε_p is proportional to $\overline{\Omega}$. This proportionality enables simple conversion from the chosen (say known – accurate and reliably determined) reference geometry (index *ref*) – to that of the actual sample (unknown efficiency)

$$\varepsilon_p \quad \varepsilon_{p,ref}\frac{\overline{\Omega}}{\overline{\Omega}_{ref}} \tag{4}$$

Note that with such conversion (*efficiency transfer* – ET), assumption of P/T constancy is practically extended (for efficiency determination) beyond its literal meaning – thanks to partial error compensation in $\overline{\Omega}\,/\,\overline{\Omega}_{ref}$ ratio. The more the actual sample and counting geometry resemble the reference ones, the more this stands.

When applying eqs. (1) and (2) to a point source T positioned above the detector (fig. 2), and a bulletized closed-end coaxial HPGe detector, we obtain

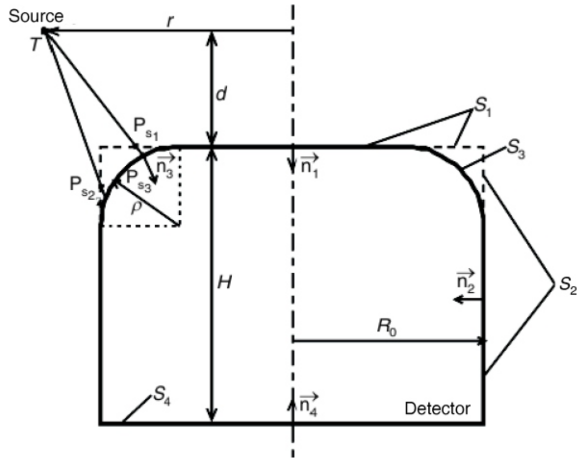

Figure 2. Point source and bulletized coaxial closed-end HPGe detector; the point is arbitrarily positioned (meaning it can vary) above the detector, while the surface of the detector is divided into portions appropriate for $\overline{\Omega}$ calculations

$$\overline{\Omega} \quad \underset{0}{\overset{2\pi}{}} \mathrm{d}\theta \underset{0}{\overset{R_0}{}} F_{att}F_{eff}\overline{F}_1(\mathrm{T},\mathrm{P}_{S_1})R\mathrm{d}R \quad \underset{\theta_0}{\overset{\theta_1}{}} R_0\,\mathrm{d}\theta \underset{H}{\overset{0}{}} F_{att}F_{eff}\overline{F}_2(\mathrm{T},\mathrm{P}_{S_2})\mathrm{d}h \tag{5}$$

with $S_D = S_1 + S_3 + S_2$ and $T(x_T, y_T, z_T)$.

Since for bulletized detectors parts of surfaces, S_1 and S_2 are *virtual* (dashed lines in fig. 2), functions $\overline{F}_1$ and $\overline{F}_2$ can be expressed as

$$\overline{F}_1(\mathrm{T},\mathrm{P}_{S_1}) \quad \begin{cases} \dfrac{\mathrm{TP}_{S_1}\ \vec{\mathrm{n}}_1}{\left|\mathrm{TP}_{S_1}\right|^3}, & R \quad R_0 \quad \rho \\ \dfrac{\mathrm{TP}_{S_3}\ \vec{\mathrm{n}}_3}{\left|\mathrm{TP}_{S_3}\right|^3}, & R \quad R_0 \quad \rho \quad \mathrm{TP}_{S_1} \quad S_3 \\ 0 \quad , & R \quad R_0 \quad \rho \quad \mathrm{TP}_{S_1} \quad S_3 \end{cases} \tag{6}$$

with $P_{S_1}(R\cos\theta, R\sin\theta, 0), \vec{\mathrm{n}}_1 \quad (0,0,\ 1), R \quad [0,R_0],$ $\theta \quad [0,2\pi], \mathrm{P}_{S_3} \quad \mathrm{TP}_{S_1} \quad S_3$ and $\vec{\mathrm{n}}_3 \quad \vec{\mathrm{n}}_3(P_{S_3})$,

$$\overline{F}_2(\mathrm{T},\mathrm{P}_{S_2}) \quad \begin{cases} \dfrac{\mathrm{TP}_{S_2}\ \vec{\mathrm{n}}_2}{\left|\mathrm{TP}_{S_2}\right|^3}, & x_T^2 \quad y_T^2 \quad R_0^2 \quad h \quad \rho \\ \dfrac{\mathrm{TP}_{S_3}\ \vec{\mathrm{n}}_3}{\left|\mathrm{TP}_{S_3}\right|^3}, & x_T^2 \quad y_T^2 \quad R_0^2 \quad h \quad \rho \quad \mathrm{TP}_{S_2} \quad S_3 \\ 0 \quad , & x_T^2 \quad y_T^2 \quad R_0^2 \quad h \quad \rho \quad \mathrm{TP}_{S_2} \quad S_3 \\ 0 \quad , & x_T^2 \quad y_T^2 \quad R_0^2 \end{cases} \tag{7}$$

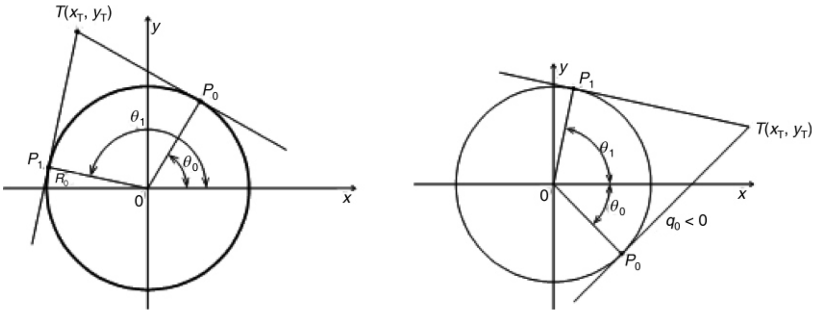

Figure 3. Integration limits for angles θ_0 and θ , encompassing the detector, as applied in eq. (8)

with $P_{S_2}\ (R_0\cos\theta, R_0\sin\theta, h), \theta\quad [\theta\quad \theta_1], h\quad H,\ 0]$, $\vec{n}_2\quad \vec{n}_2(P_{S_2})\quad (\ \cos\theta,\ \sin\theta, 0)$, and $P_{S_3}\quad TP_{S_2}\quad S_3$ and $\vec{n}_3\quad \vec{n}_3(P_{S_3})$.

For angles θ and θ (fig. 3) we have

$$\theta_{0,1}\quad \begin{matrix} \arccos\hat{x}_{0,1}, & \hat{y}_{0,1}\quad 0 \\ 2\pi\quad \arccos\hat{x}_{0,1}, & \hat{y}_{0,1}\quad 0 \end{matrix}$$

with

$$\hat{x}_{0,1}\quad \frac{R_0|x_T| \mp y_T\sqrt{x_T^2\quad y_T^2\quad R_0^2}}{x_T^2\quad y_T^2}\ \operatorname{sgn} x_T$$

and

$$\hat{y}_{0,1}\quad \frac{R_0 y_T\quad |x_T|\ \sqrt{x_T^2\quad y_T^2\quad R_0^2}}{x_T^2\quad y_T^2}$$

Note that if $x_T = 0$ (point T at Oy-axis) then

$$\hat{y}_0\quad \hat{y}_1\quad \frac{R_0^2}{y_T}\ \text{and}\ \hat{x}_{0,1}\quad \mp\frac{\sqrt{R_0^2\quad \hat{y}_{0,1}^2}}{R_0}$$

For coaxial *brick* geometry (fig. 4), we consequently obtain a generally applicable formula

$$\overline{\Omega}\quad \frac{1}{abL}\int_0^L \mathrm{d}l \int_{\frac{a}{2}}^{\frac{a}{2}} \mathrm{d}x \int_{\frac{a}{2}}^{\frac{a}{2}} \mathrm{d}y \int_0^{2\pi} \mathrm{d}\theta \int_0^{R_0} F_{\text{att}} F_{\text{eff}} \overline{F}_1(T, P_{S_1}) R\,\mathrm{d}R$$
$$R_0 \int_{\theta_0}^{\theta_1} \mathrm{d}\theta \int_{H}^{0} F_{\text{att}} F_{\text{eff}} \overline{F}_2(T, P_{S_2})\,\mathrm{d}h \qquad (8)$$

with $T\,(x_0 + x, y_0 + y, d + l\,)$, where x_0 and y_0 are axial displacements of the source (fig. 5).

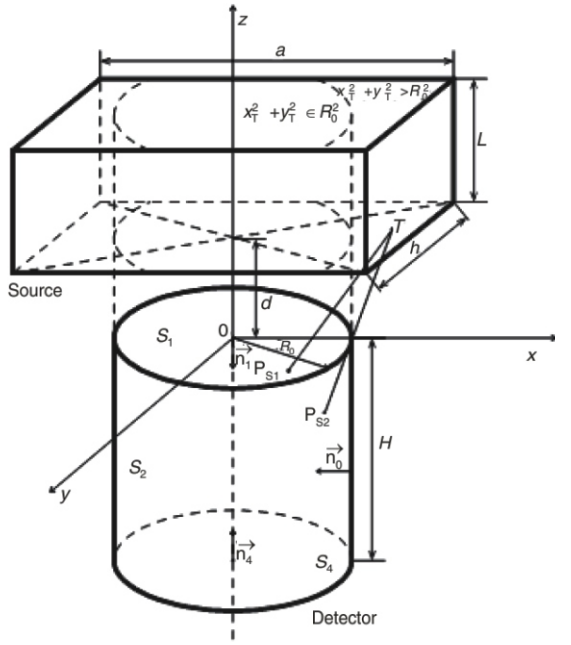

Figure 4. ***Brick*** **geometry; cylindrical detector and brick source are coaxially positioned, their**

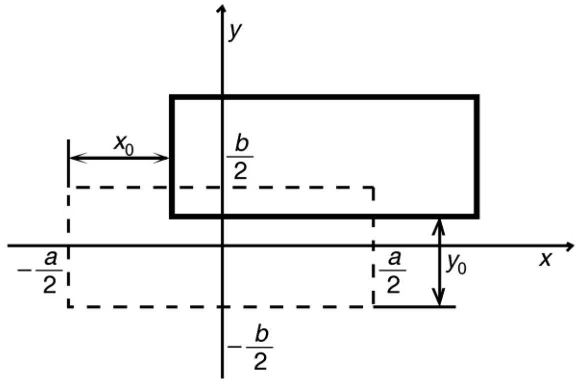

Figure 5. Axial displacement of the brick source, as seen from z-axis; bases of the detector and the source are still plane-parallel, but are not coaxial (full line denotes the base of the displaced source, while the dashed line is of the coaxial one)

NUMERICAL TESTING

So as to get a preliminary idea about the reliability and accuracy of the model, we compared it to previously/independently developed and well established/tested model of cylindrical sources. Namely, a brick-shape source can be understood as interpolation between the corresponding outer and inner cylinders (fig. 6). By suitably varying dimensions and proportions of these, one can obtain a fair idea about the reliability (absence of systematic errors) and accuracy of the model. Also, by setting the source height to zero, it can be compared with previous models of disk-shape and point sources, as follows.

For the sake of completeness, we also tested brick-shape source *vs*. a cylindrical source, its axis being positioned with an axial shift *vs.* the detector axis (axial displacement, fig. 5).

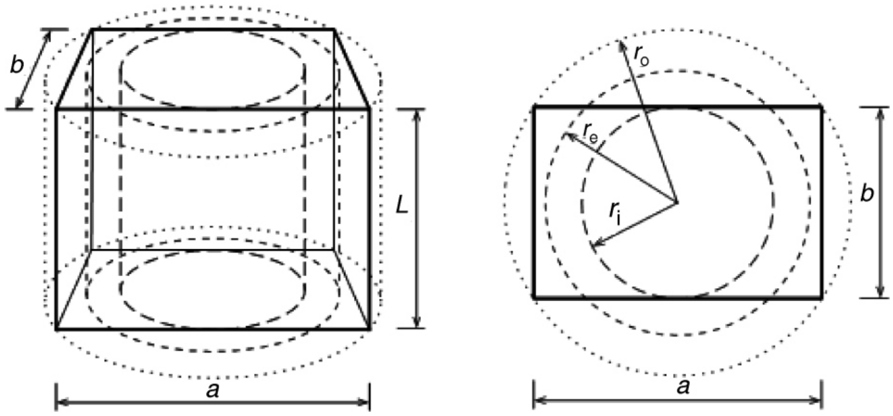

Figure 6. To the numerical testing of the model: brick source with inner (r_i), outer (r_0), and *equivoluminous* (r_e) cylinders (left: perspective view, right: vertical projection)

Parameters of the semiconductor detector chosen for numerical testing are given in tab. 1, and illustrated in fig. 7.

Source parameters are set to vary as follows:

width: b = 1 cm, 2.5 cm, 5 cm and 7 cm,

length: a = b, 1.5 b, 2 b,

height: L = 0 cm, 0.1 cm, 1 cm and 5 cm,

(L = 0 accounts for the infinitely thin slab),

with gamma energies of interest: 50, 100, 500, 1000, and 3000 keV.

Results are presented in both numerical form (tab. 2) and graphically (fig. 8). Table 2 shows the effective solid angles for each chosen brick source and corresponding inner, outer and *equivoluminous* cylinder (with radii r_i, r_o, and r_e, respectively), and for 5 gamma energies from the specified range. In fig. 8 the same is shown in graphical form, so as to more easily perceive the results and make conclusions. Also, the characteristic dependence of the effective solid angles (and hence, consequently to eq. (3), of the detection efficiencies as well) on gamma energies can be observed.

Two sets of results are shown: for b = 2.5 cm and b = 7 cm. Note that for given value of b (brick width), the radius of inner cylinder is $r_i = b/2$ for every brick length; r_i is therefore given in the first column of the table (shaded). The other 3 groups of 3 columns each show results for $a = b$, $a = 1.5\,b$ and $a = 2\,b$, respectively. For visual clarity, the middle ones (for a = 1.5 b) are shaded.

Obviously, the results are exactly as expected: effective solid angles (thus, detection efficiencies as well) for brick sources lay consistently, with no exception, between those of corresponding inner and outer cylinders, while close to equivoluminous cylinders. This clearly and conclusively indicates that the brick model is free of systematic errors (bugs), thus being accurate and reliable.

Table 1. The parameters of the semiconductor detector chosen for numerical testing

Detector parameter	Value [mm]
Crystal radius	25
Crystal height	60
Crystal hole radius	4
Crystal hole heigh	40
Crystal bulletization radius	4
Al cap thickness (top)	0.5
Al cap thickness (side)	1
Vacuum (top and side)	3
Dead layer (top and side)	0.6
Contact	0.001

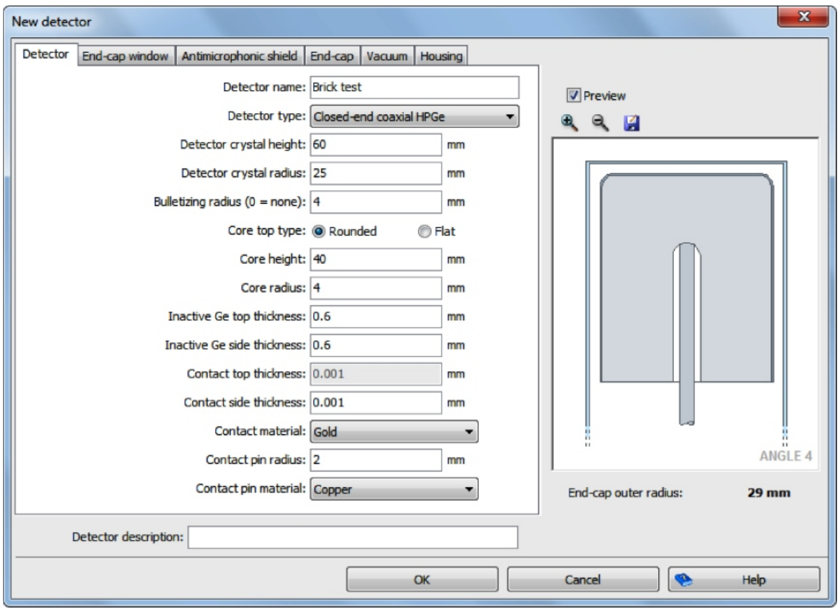

Figure 7. Parameters of the semiconductor detector chosen for numerical testing, illustration to tab. 1; screenshot from software [12]

Table 2. Effective solid angles for brick sources with the dimensions *a* [cm], *b* [cm], and *L* [cm], compared to inner cylinders (radius r_i), outer cylinders (radius r_o), and *equivoluminous* cylinders (radius r_e) (fig. 6); all for coaxial positioning and with axial displacement (fig. 5); gamma energy range 50-3000 keV

Source width: b = 2.5 cm

Source and detector are coaxial: $x_0 = 0$, $y_0 = 0$											
	E_γ	r_i = 1.25	a = 2.5	r_e = 1.4105	r_o = 1.7678	a = 3.75	r_e = 1.7275	r_o = 2.2535	a = 5	r_e = 1.9947	r_o = 2.7951
L = 5 cm	50	0.30864	0.29793	0.29768	0.27421	0.27343	0.27680	0.24190	0.24590	0.25932	0.20478
	100	0.98608	0.95572	0.95583	0.89017	0.88704	0.89747	0.79915	0.80980	0.84824	0.69564
	500	0.84148	0.82349	0.82431	0.78566	0.78246	0.79018	0.72965	0.73294	0.76030	0.66174
	1000	0.73993	0.72593	0.72694	0.69685	0.69370	0.70051	0.65200	0.65336	0.67672	0.59617
	3000	0.57905	0.56974	0.57080	0.55073	0.54796	0.55333	0.51958	0.51925	0.53692	0.47938
L = 1 cm	50	0.68651	0.67235	0.67443	0.63849	0.62707	0.64330	0.56161	0.55399	0.60678	0.45713
	100	2.40306	2.34558	2.35361	2.21966	2.18696	2.23662	1.97252	1.96023	2.11362	1.65843
	500	1.96996	1.92912	1.93560	1.84509	1.82558	1.85700	1.68909	1.67978	1.77727	1.48640
	1000	1.68418	1.65122	1.65677	1.58407	1.56856	1.59403	1.45945	1.45073	1.52988	1.29491
	3000	1.27085	1.24772	1.25190	1.20111	1.19044	1.20850	1.11469	1.10736	1.16352	0.99798
L = 0.1 cm	50	0.83305	0.82803	0.82899	0.80904	0.79127	0.81250	0.72345	0.69644	0.77980	0.57872
	100	3.25670	3.20224	3.21291	3.07353	3.01488	3.09294	2.73366	2.67621	2.93938	2.24677
	500	2.73098	2.67709	2.68831	2.56467	2.53062	2.58146	2.33052	2.30180	2.46651	2.00537
	1000	2.31101	2.26677	2.27674	2.17558	2.14847	2.18966	1.98740	1.96440	2.09622	1.72321
	3000	1.72023	1.68879	1.69671	1.62485	1.60580	1.63523	1.49313	1.47701	1.56887	1.30509
L = 0	50	0.84861	0.84542	0.84555	0.82901	0.81100	0.83202	0.74494	0.71380	0.80196	0.59488
	100	3.37770	3.32615	3.33577	3.19967	3.13790	3.21883	2.85048	2.78152	3.06526	2.33382
	500	2.85229	2.79792	2.80940	2.67961	2.64288	2.69834	2.43220	2.40070	2.57751	2.08846
	1000	2.41056	2.36583	2.37651	2.26888	2.23976	2.28500	2.06896	2.04557	2.18605	1.79135
	3000	1.79123	1.75932	1.76833	1.69034	1.67012	1.70261	1.54918	1.53485	1.63162	1.35333
Source axially displaced: $x_0 = 0.8$, $y_0 = 0.6$											
	E_γ	r_i = 1.25	a = 2.5	r_e = 1.4105	r_o = 1.7678	a = 3.75	r_e = 1.7275	r_o = 2.2535	a = 5	r_e = 1.9947	r_o = 2.7951
L = 5 cm	50	0.28276	0.27198	0.27196	0.24914	0.24924	0.25162	0.22121	0.22810	0.23570	0.19263
	100	0.91041	0.88080	0.88118	0.81870	0.81893	0.82548	0.74216	0.76176	0.78185	0.66421
	500	0.79189	0.77432	0.77512	0.73795	0.73693	0.74211	0.69122	0.70140	0.71568	0.64129
	1000	0.69889	0.68517	0.68613	0.65716	0.65571	0.66048	0.61989	0.62707	0.63953	0.57919
	3000	0.54915	0.53997	0.54098	0.52168	0.52002	0.52398	0.49596	0.49995	0.50966	0.46701
L = 1 cm	50	0.62145	0.60005	0.60253	0.55645	0.55157	0.56167	0.49614	0.50368	0.52780	0.42801
	100	2.17407	2.10665	2.11461	1.97164	1.95842	1.98772	1.78364	1.81085	1.88262	1.57442
	500	1.81509	1.77315	1.77784	1.68823	1.67972	1.69844	1.56982	1.58458	1.63264	1.43170
	1000	1.55888	1.52550	1.52912	1.45770	1.45054	1.46591	1.36258	1.37378	1.41333	1.24997
	3000	1.18253	1.15947	1.16185	1.11244	1.10711	1.11819	1.04582	1.05312	1.08167	0.96548
L = 0.1 cm	50	0.77925	0.75285	0.75605	0.69496	0.69075	0.70154	0.62938	0.63494	0.66200	0.54891
	100	2.97468	2.87881	2.89245	2.68358	2.66495	2.70638	2.43321	2.46207	2.56229	2.14073
	500	2.50646	2.44195	2.44941	2.30640	2.30131	2.32198	2.14836	2.15983	2.23012	1.94276
	1000	2.12905	2.07736	2.08249	1.96625	1.96455	1.97896	1.84369	1.85043	1.90735	1.67664
	3000	1.59221	1.55620	1.55894	1.47625	1.47745	1.48535	1.39495	1.39738	1.43751	1.27658
L = 0	50	0.79907	0.77179	0.77501	0.70981	0.70807	0.71666	0.64685	0.65162	0.67705	0.56617
	100	3.09522	2.99399	3.00834	2.78438	2.76909	2.80846	2.53019	2.55850	2.65919	2.22745
	500	2.61852	2.54930	2.55798	2.40092	2.40004	2.41668	2.24098	2.25082	2.32205	2.02570
	1000	2.22083	2.16534	2.17173	2.04328	2.04557	2.05589	1.92035	1.92517	1.98254	1.74559
	3000	1.65750	1.61883	1.62281	1.53067	1.53515	1.53948	1.45020	1.45065	1.49080	1.32654
Source axially displaced: $x_0 = 0.5$, $y_0 = 0$											
	E_γ	r_i = 1.25	a = 2.5	r_e = 1.4105	r_o = 1.7678	a = 3.75	r_e = 1.7275	r_o = 2.2535	a = 5	r_e = 1.9947	r_o = 2.7951
L = 5 cm	50	0.30230	0.29150	0.29129	0.24914	0.26689	0.27022	0.23510	0.24183	0.25244	0.20036
	100	0.96727	0.93697	0.93712	0.81870	0.86858	0.87877	0.78105	0.79945	0.82926	0.68569
	500	0.82875	0.81125	0.81182	0.73795	0.76991	0.77796	0.71702	0.72643	0.74759	0.65544
	1000	0.72931	0.71580	0.71655	0.65716	0.68318	0.69039	0.64143	0.64797	0.66617	0.59098
	3000	0.57124	0.56236	0.56319	0.52168	0.54019	0.54596	0.51181	0.51533	0.52923	0.47565
L = 1 cm	50	0.67228	0.65499	0.65806	0.61582	0.60535	0.62137	0.53749	0.54348	0.58128	0.44599
	100	2.34874	2.28635	2.29591	2.15264	2.12328	2.17067	1.90760	1.93148	2.04293	1.63248
	500	1.92920	1.89010	1.89530	1.80409	1.78494	1.81589	1.64477	1.66229	1.73334	1.47072
	1000	1.65008	1.61982	1.62349	1.55141	1.53542	1.56093	1.42293	1.43657	1.49472	1.28247
	3000	1.24574	1.22575	1.22776	1.17856	1.16680	1.18527	1.08837	1.09734	1.13914	0.98947
L = 0.1 cm	50	0.82689	0.81234	0.81883	0.77509	0.75928	0.78200	0.66878	0.68393	0.72883	0.54990
	100	3.19929	3.12631	3.14646	2.96311	2.91076	2.98866	2.59250	2.63727	2.79957	2.18312
	500	2.67426	2.61722	2.63317	2.49335	2.46506	2.51368	2.22147	2.27749	2.37292	1.94908
	1000	2.26309	2.21776	2.23130	2.11791	2.09557	2.13515	1.89282	1.94428	2.01839	1.67272
	3000	1.68476	1.65379	1.66394	1.58399	1.56848	1.59692	1.42007	1.46215	1.51164	1.26482
L = 0	50	0.84515	0.83021	0.83845	0.79259	0.77791	0.80010	0.67870	0.70109	0.74232	0.55802
	100	3.32332	3.24833	3.27206	3.07993	3.02696	3.10739	2.68121	2.74083	2.90313	2.25290
	500	2.79721	2.73346	2.75586	2.60133	2.57508	2.62484	2.30236	2.37420	2.46789	2.01253
	1000	2.36475	2.31260	2.33317	2.20599	2.18579	2.22637	1.95786	2.02329	2.09528	1.72363
	3000	1.75802	1.72082	1.73783	1.64632	1.63268	1.66204	1.46520	1.51808	1.56547	1.30018

Source width: b = 7 cm

Source axially displaced: $x_0 = 0$, $y_0 = 0$

	E_γ	$r_i = 3.5$	$a = 7$	$r_e = 3.9493$	$r_o = 4.9497$	$a = 10.5$	$r_e = 4.8369$	$r_o = 6.3097$	$a = 14$	$r_e = 5.5852$	$r_o = 7.8262$
L = 5 cm	50	0.16465	0.14327	0.14436	0.11143	0.11200	0.11445	0.08403	0.09277	0.09681	0.06557
	100	0.58820	0.52957	0.53327	0.43880	0.43757	0.44793	0.34972	0.37210	0.39295	0.28071
	500	0.59237	0.54887	0.55312	0.47638	0.47175	0.48366	0.39239	0.40892	0.43500	0.32230
	1000	0.53913	0.50209	0.50603	0.43941	0.43474	0.44546	0.36428	0.37861	0.40284	0.30132
	3000	0.43830	0.41046	0.41372	0.36249	0.35832	0.36683	0.30269	0.31378	0.33381	0.25251
L = 1 cm	50	0.35228	0.30179	0.30327	0.23063	0.23320	0.23699	0.17492	0.19428	0.20061	0.13796
	100	1.35160	1.19317	1.20120	0.95488	0.95563	0.97802	0.73700	0.79873	0.84107	0.57776
	500	1.28830	1.16730	1.17660	0.96891	0.96207	0.98952	0.76178	0.81124	0.86312	0.60055
	1000	1.13360	1.03156	1.03960	0.86052	0.85379	0.87843	0.67855	0.72116	0.76784	0.53585
	3000	0.88301	0.80724	0.81322	0.67669	0.67096	0.69046	0.53514	0.56771	0.60479	0.42340
L = 0.1 cm	50	0.44360	0.38150	0.38367	0.29640	0.29508	0.30423	0.22816	0.24995	0.26012	0.18165
	100	1.79680	1.57326	1.58370	1.24410	1.24084	1.27620	0.95167	1.03701	1.09150	0.74274
	500	1.70410	1.52139	1.53430	1.23520	1.22045	1.26460	0.95243	1.02340	1.08960	0.74134
	1000	1.48000	1.32485	1.33610	1.07950	1.06445	1.10510	0.83297	0.89332	0.95261	0.64833
	3000	1.13410	1.01783	1.02640	0.83207	0.81871	0.85181	0.64228	0.68755	0.73441	0.49980
L = 0	50	0.45660	0.39264	0.39521	0.30645	0.30249	0.31437	0.23650	0.25831	0.26939	0.18860
	100	1.86245	1.62856	1.63951	1.28724	1.27901	1.32030	0.98406	1.07231	1.12920	0.76811
	500	1.76546	1.57267	1.58774	1.27467	1.25437	1.30490	0.98037	1.05415	1.12555	0.76297
	1000	1.52864	1.36607	1.37949	1.11081	1.09093	1.13760	0.85507	0.91770	0.98225	0.66534
	3000	1.16655	1.04615	1.05653	0.85308	0.83609	0.87441	0.65713	0.70403	0.75545	0.51107

Source axially displaced: $x_0 = 0.8$ cm, $y_0 = 0.6$ cm

	E_γ	$r_i = 3.5$	$a = 7$	$r_e = 3.9493$	$r_o = 4.9497$	$a = 10.5$	$r_e = 4.8369$	$r_o = 6.3097$	$a = 14$	$r_e = 5.5852$	$r_o = 7.8262$
L = 5 cm	50	0.15877	0.13987	0.14060	0.11023	0.11062	0.11314	0.08356	0.09208	0.09582	0.06517
	100	0.57169	0.51835	0.52134	0.43300	0.43169	0.44182	0.34675	0.36851	0.38828	0.27882
	500	0.57738	0.53691	0.54055	0.46935	0.46485	0.47697	0.38954	0.40450	0.42937	0.31999
	1000	0.52588	0.49116	0.49467	0.43293	0.42837	0.43963	0.36202	0.37446	0.39769	0.29919
	3000	0.42794	0.40156	0.40461	0.35719	0.35307	0.36240	0.30123	0.31029	0.32967	0.25078
L = 1 cm	50	0.34242	0.29675	0.29861	0.22919	0.23115	0.23547	0.17411	0.19388	0.19956	0.13746
	100	1.31415	1.16797	1.17653	0.94303	0.94322	0.96555	0.73141	0.79230	0.83285	0.57493
	500	1.24958	1.13645	1.14762	0.95500	0.94702	0.97510	0.75675	0.80328	0.85458	0.59900
	1000	1.09930	1.00313	1.01365	0.84835	0.84016	0.86587	0.67468	0.71411	0.76077	0.53502
	3000	0.85611	0.78387	0.79273	0.66737	0.66001	0.68087	0.53271	0.56222	0.59977	0.42327
L = 0.1 cm	50	0.43471	0.37790	0.37968	0.29482	0.29284	0.30240	0.22737	0.25276	0.25880	0.18134
	100	1.75139	1.54413	1.55462	1.23080	1.22577	1.26146	0.94611	1.03528	1.08177	0.74033
	500	1.65240	1.48281	1.49761	1.21979	1.20326	1.24895	0.94735	1.02208	1.08085	0.74068
	1000	1.43444	1.28980	1.30377	1.06606	1.04921	1.09158	0.82914	0.89331	0.94581	0.64830
	3000	1.09869	0.98967	1.00140	0.82182	0.80672	0.84157	0.63994	0.68874	0.72998	0.50026
L = 0	50	0.44749	0.39008	0.39115	0.30476	0.30062	0.31228	0.23557	0.26211	0.26793	0.18830
	100	1.81593	1.60047	1.61007	1.27372	1.26442	1.30499	0.97836	1.07269	1.11910	0.76566
	500	1.71233	1.53570	1.54816	1.25827	1.23763	1.28841	0.97453	1.05482	1.11393	0.76147
	1000	1.48287	1.33293	1.34413	1.09663	1.07625	1.12305	0.85027	0.91937	0.97208	0.66438
	3000	1.13226	1.02003	1.02887	0.84246	0.82477	0.86293	0.65372	0.70639	0.74772	0.51068

Source axially displaced: $x_0 = 0.5$ cm, $y_0 = 0$

	E_γ	$r_i = 3.5$	$a = 7$	$r_e = 3.9493$	$r_o = 4.9497$	$a = 10.5$	$r_e = 4.8369$	$r_o = 6.3097$	$a = 14$	$r_e = 5.5852$	$r_o = 7.8262$
L = 5 cm	50	0.16288	0.14243	0.14327	0.11097	0.11222	0.11396	0.08381	0.09290	0.09649	0.06544
	100	0.58351	0.52673	0.53003	0.43708	0.43715	0.44608	0.34878	0.37186	0.39164	0.28018
	500	0.58841	0.54580	0.54985	0.47447	0.47086	0.48220	0.39198	0.40817	0.43331	0.32155
	1000	0.53577	0.49928	0.50313	0.43765	0.43383	0.44442	0.36420	0.37777	0.40119	0.30054
	3000	0.43583	0.40817	0.41144	0.36103	0.35749	0.36628	0.30293	0.31294	0.33235	0.25176
L = 1 cm	50	0.34793	0.30060	0.30083	0.22943	0.23500	0.23572	0.17421	0.19512	0.19963	0.13750
	100	1.33867	1.18680	1.19267	0.95053	0.95688	0.97326	0.73463	0.79908	0.83771	0.57641
	500	1.27656	1.15931	1.16850	0.96574	0.96194	0.98586	0.76086	0.81081	0.86112	0.60084
	1000	1.12386	1.02417	1.03307	0.85842	0.85333	0.87586	0.67845	0.72074	0.76684	0.53672
	3000	0.87607	0.80115	0.80887	0.67578	0.67022	0.68916	0.53581	0.56737	0.60481	0.42469
L = 0.1 cm	50	0.43061	0.38074	0.37432	0.29076	0.30578	0.29809	0.22477	0.25333	0.25542	0.17950
	100	1.76521	1.56582	1.56080	1.23154	1.25811	1.26187	0.94429	1.04151	1.08081	0.73824
	500	1.66665	1.51118	1.50917	1.22217	1.23991	1.24913	0.94509	1.03160	1.07912	0.73815
	1000	1.44468	1.31568	1.31348	1.06749	1.08281	1.09079	0.82669	0.90224	0.94354	0.64575
	3000	1.10437	1.01063	1.00838	0.82224	0.83401	0.84015	0.63761	0.69618	0.72748	0.49796
L = 0	50	0.43900	0.39207	0.38208	0.38238	0.31806	0.30581	0.23161	0.30581	0.26269	0.18561
	100	1.82108	1.62099	1.60835	1.60927	1.30611	1.30093	0.97345	1.30093	1.11429	0.76176
	500	1.71926	1.56291	1.55475	1.55527	1.28473	1.28426	0.96958	1.28426	1.10860	0.75717
	1000	1.48715	1.35758	1.35044	1.35094	1.11973	1.11872	0.84572	1.11872	0.96675	0.66039
	3000	1.13399	1.03976	1.03433	1.03477	0.86037	0.85914	0.65010	0.85914	0.74300	0.50743

Results for the point sources, compared to those of very small (*quasi point*) voluminous ones are given in tab. 3, illustrating the convergence. Note that the results for the point sources are exactly the same when obtained by two different calculation approaches – as infinitely small bricks ($a = 0$, $b = 0$, $L = 0$) or infinitely small cylinders ($r = 0$, $L = 0$). Again, sources both coaxially positioned and with axial displacement were considered.

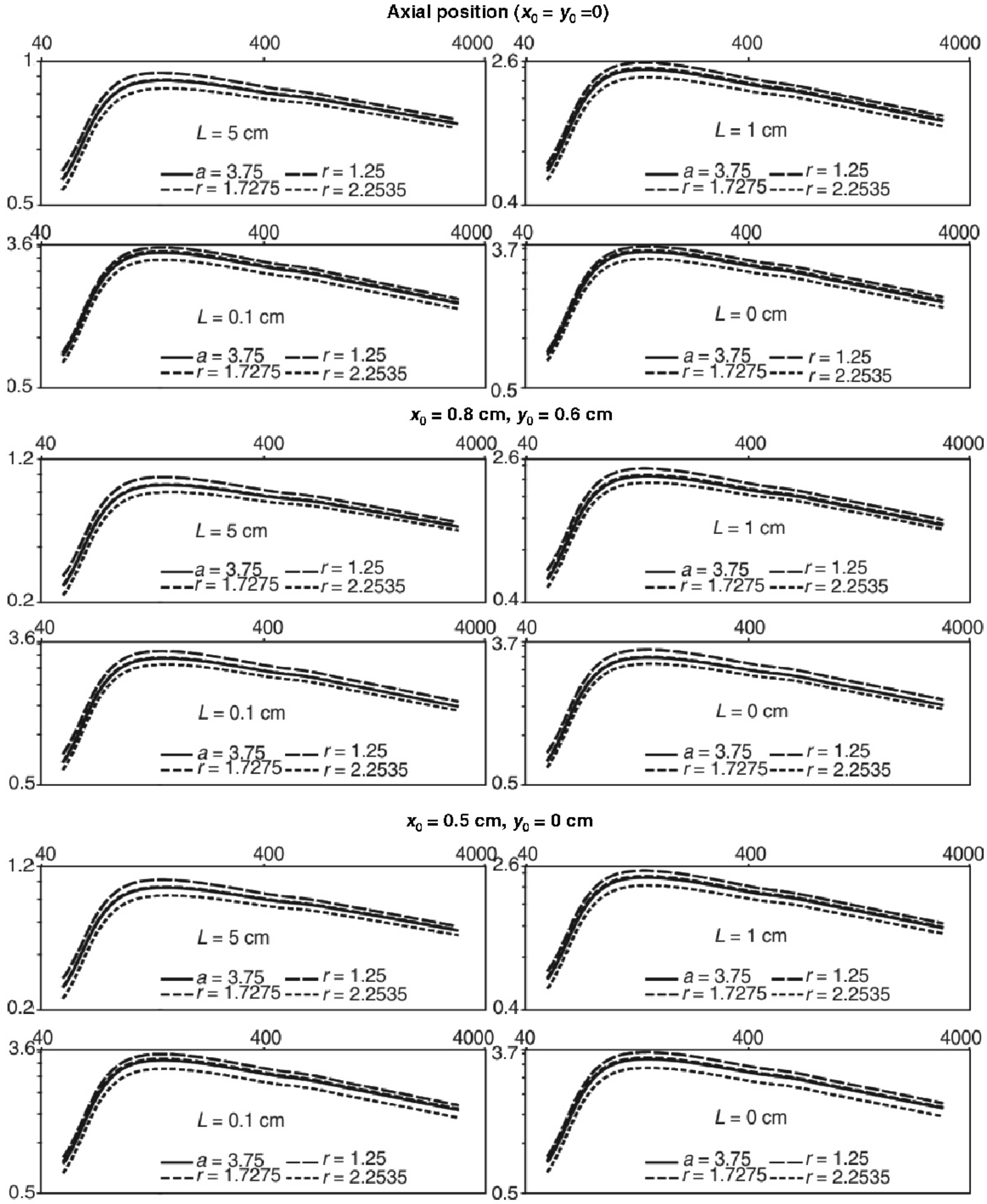
Axial position (x_0 = y_0 =0)
x_0 = 0.8 cm, y_0 = 0.6 cm
x_0 = 0.5 cm, y_0 = 0 cm
L = 5 cm
L = 1 cm
L = 0.1 cm
L = 0 cm
a = 3.75
r = 1.25
r = 1.7275
r = 2.2535

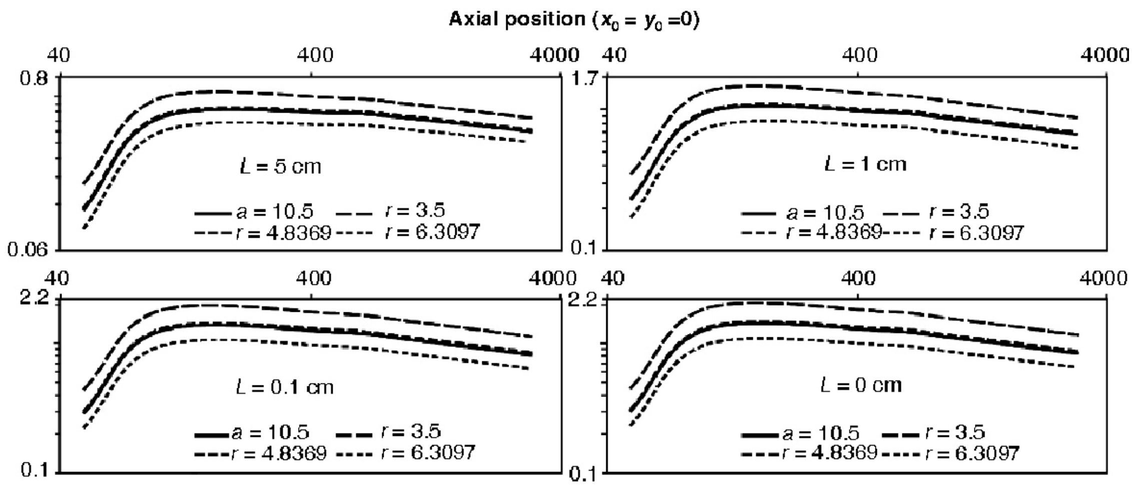
Axial position (x_0 = y_0 =0)
L = 5 cm
L = 1 cm
L = 0.1 cm
L = 0 cm
a = 10.5
r = 3.5
r = 4.8369
r = 6.3097

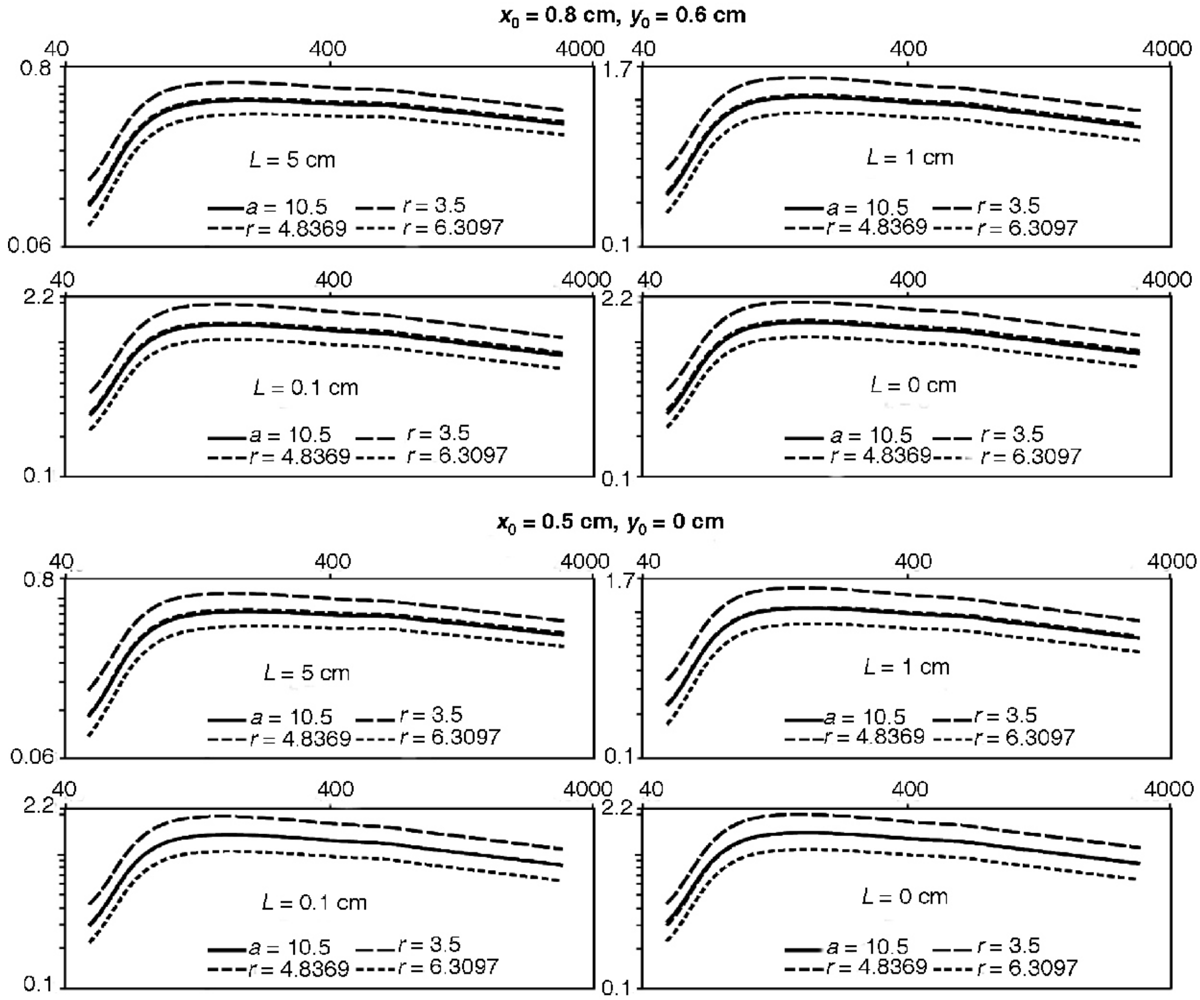

Figure 8. Graphical representation of results given in tab. 2; effective solid angles *vs*. gamma-energies (in keV) for various brick source dimensions

Table 3. Effective solid angles for point sources compared to those for very small bricks and cylinders; coaxial positioning (shaded) and with the axial displacement, illustrating the convergence

	E_γ	a = 0.01 b = 0.01 L = 0.01	a = 0 b = 0 L = 0	r = 0 L = 0	a = 0.01 b = 0.01 L = 0.01 x_0 = 0.8 y_0 = 0.6	a = 0 b = 0 L = 0 x_0 = 0.8 y_0 = 0.6	r = 0 L = 0 x_0 = 1
d = 0	50	0.852166	0.852932	0.852932	0.847097	0.847978	0.847978
	100	3.48502	3.49343	3.49343	3.33878	3.34820	3.34820
	500	2.99086	3.00200	3.00200	2.79520	2.80634	2.80634
	1000	2.52477	2.53398	2.53398	2.36050	2.36982	2.36982
	3000	1.87252	1.87904	1.87904	1.75205	1.75880	1.75880
d = 6	50	0.119950	0.120353	0.120353	0.115835	0.116220	0.116220
	100	0.296510	0.297385	0.297385	0.288876	0.289722	0.289722
	500	0.247922	0.248460	0.248460	0.243337	0.243863	0.243863
	1000	0.215028	0.215434	0.215434	0.211302	0.211701	0.211701
	3000	0.165110	0.165366	0.165366	0.162445	0.162698	0.162698
d = 12	50	0.0361105	0.0362593	0.0362593	0.0357064	0.0358533	0.0358533
	100	0.0890196	0.0893234	0.0893234	0.0882380	0.0885389	0.0885389
	500	0.0815678	0.0817530	0.0817530	0.0809373	0.0811203	0.0811203
	1000	0.0721044	0.0722374	0.0722374	0.0715614	0.0716925	0.0716925
	3000	0.0565211	0.0565969	0.0565969	0.0561084	0.0561826	0.0561826

Besides the above numerical testing, in a separate paper to follow, we will also report on the experimental verification of the model.

APPLICABILITY

It was the applicability of the brick-shape counting geometry which drove us towards the development of the above mathematical model. This includes *i. a*., low radioactivity measurements of:

- environmental samples,
- food packages (milk and diary products, canned meat, fish, ready meals, food, *etc*.),
- forage (*e. g*., hay or straw bales),
- brick-shape packages of general consumables (*e. g*. cosmetics, household items),
- construction materials (bricks of clay, concrete or composites, stone cuts, ceramics, metal profiles and ingots, *etc*.),
- some forms of radioactive waste (medical, industrial from scientific research, *etc*.), brick-shape compressed,
- whole body counting models/phantoms, *etc*.

The brick source measurements can be part of routine monitoring programs or regulatory control procedures. They can also be used for emergency preparedness or in the aftermath of major radiological accidents (crisis management), when huge numbers of various types of samples (mainly food and environmental samples) need to be analyzed for contamination under time constraints.

CONCLUSIONS

A mathematical model of rectangular cuboid (brick-shape) sources for semiconductor detector gamma-efficiency calculations is elaborated and presented in detail in this work. Brick-shape sources with no limitation (full flexibility) in size, proportion, matrix composition, container, *etc*. are considered. With one of its sides plane-parallel to the detector top surface, sources can be positioned with their centre either on or off the detector crystal axis. Testing is made by numerical calculation comparisons to previously/independently developed and well established models of cylindrical sources. Selected results of the testing are shown in both tabular and graphical form, convincingly illustrating the reliability of the model.

Practical applications include routine measurements (*e. g*., of food, environmental samples, or construction materials) – for regulatory control, emergency preparedness or radiological accident aftermath situations – saving on laboratory time and reducing the potential for systematic errors in analytical tasks.

The model is expected to be available as a part of ANGLE software for advanced quantitative gamma-spectrometry. Extension to scintillation detectors (NaI, $LaBr_3$, *etc*.) is simple and straightforward – the scintillation detectors technically being regarded as a *simplified* variation of semiconductor ones – thus not deemed to be elaborated separately in this paper; the extension, however, will be available as a separate option in ANGLE as well.

AUTHORS' CONTRIBUTIONS

N. N. Mihaljevic developed the mathematical model presented in the paper and performed numerical testing. S. I. Jovanovic conceived and wrote the paper. A. D. Dlabac and M. S. Badawi made valuable contributions in various phases of the work. All authors extensively interacted, exchanging the ideas, especially during the preparation of the manuscript.

REFERENCES

[1] Nafee, S. S., Abbas, M. I., Calibration of Closed-end HPGe Detectors Using Bar (Parallelepiped) Sources, *Nucl. Instrum. Methods Phys. Res. A, 592* (2008), 1-2, pp. 80-87

[2] Gouda, M. M, *et al*., New Analytical Approach to Calculate the Co axial HPGe Detector Efficiency Using Parallelepiped Sources, *J. Adv. Res. Phys., 4* (2013), 1, ID 011303

[3] El-Khatib, A. M., *et al*., Calculation of Full Energy Peak Efficiency of NaI (Tl) Detectors by New Analytical Approach for Parallelepiped Sources, *J. Theor. Appl. Phys., 7* (2013), 1, pp. 1-11

[4] Badawi, M. S., *et al*., A New Mathematical Model for Determining Full Energy Peak Efficiency of an Array of Two Gamma Detectors Counting Rectangular Parallelepiped Sources, *Nucl Technol Radiat, 28* (2013), 4, pp. 370-380

[5] Badawi, M. S., *et al*., NaI(Tl) Detector Efficiency Computation Using Radioactive Parallelepiped Sources Based on Efficiency Transfer Principle, *Sci. Technol. Nucl. Installat., 2015* (2015), ID 451932

[6] Moens, J., *et al*., Calculation of the Absolute Peak Efficiency of Gamma Ray Detectors for Different Counting Geometries, *Nucl. Instr. Meth., 187* (1981), 2-3, pp. 451-472

[7] Moens, J., *et al*., Calculation of the Absolute Peak Efficiency of Ge and Ge(Li) Detectors for Different Counting Geometries, *J. Radioanal. Nucl. Chem., 70* (1982), 1-2, pp. 539-550

[8] Moens, L., Hoste, J., Calculation of the Peak Efficiency of High Purity Germanium Detectors, *Internat. J. Appl. Radiat. Isot., 34* (1983), 8, pp. 1085-1095

[9] Gouda, M. M., *et al*., Calculation of the NaI(Tl) Detector Full-Energy Peak Efficiency Using the Efficiency Transfer Method for Small Radioactive Cylindrical Sources, *Nucl Technol Radiat, 31* (2016), 2, pp. 150-158

[10] Mihaljevic, N., *et al*., Accounting for Detector Crystal Edge Rounding (Bulletization) in Gamma Efficiency Calculations – Theoretical Elaboration and Practical Application in ANGLE Software, *Nucl Technol Radiat, 27* (2012), 1, pp. 1-12

[11] Vukotic, P., *et al*., On the Applicability of the Effective Solid Angle Concept in Activity Determination of Large Cylindrical Sources, *J. Radioanal. Nucl. Chem., 218* (1997), 1, pp. 21-28

[12] ***, ANGLE 4 – Advanced Gamma Spectrometry Software, http://angle4.com
[13] Andreev, D. S., *et al*., Consideration of Cascade Transitions in Determining the Absolute Yield of Gamma Rays, *Instr. Expt. Techn., 15* (1972), 9, pp. 1358-1359
[14] Mihaljevic, N., *et al*., "EXTSANGLE" – An Extension of the Efficiency Conversion Program "SOLANG" to Sources with a Diameter Larger than that of the Ge Detector, *J. Radioanal. Nucl. Chem., 169* (1993), 1, pp. 209-218
[15] Erten, H. N., *et al*., Efficiency Calibration and Summation Effects in Gamma Ray Spectrometry, *J. Radioanal. Nucl. Chem., 125* (1988), 1, pp. 3-10

Received on October 19, 2017
Accepted on April 12, 2018

**Никола Н. МИХАЉЕВИЋ, Слободан И. ЈОВАНОВИЋ,
Александар Д. ДЛАБАЧ, Мохамед С. БАДАВИ**

МАТЕМАТИЧКИ МОДЕЛ КАЛИБРАЦИЈЕ ГАМА-ЕФИКАСНОСТИ ПОЛУПРОВОДНИЧКИХ ДЕТЕКТОРА ЗА ИЗВОРЕ У ОБЛИКУ КВАДРА

Радиоактивни извори у облику квадра (правоуглог паралелопипеда) не срећу се баш често у полупроводничкој гама-спектрометрији, где се претежно ради са аксијално симетричним изворима. Међутим, у неким посебним случајевима, као што је контрола радиоактивности у храни или грађевинским материјалима (у циљу мониторинга или регулаторне контроле извора зрачења, као и у ситуацијама након нуклеарних/радиолошких акцидената), извори у облику квадра могу доћи до изражаја. Да би се поједноставила рутинска/репетитивна мерења таквих извора ниских активности, лакше је и практичније мерити их у њиховом оригиналном облику (квадар), то јест, не претварати их у неки "правилнији", тј. више уобичајен облик (цилиндрични или Маринели). Овим се значајно штеде време, рад и потрошни материјал, те у коначном смањује трошак и повећава учинак лабораторије. Такође се побољшава поузданост добијених аналитичких резултата, јер се смањује могућност прављења систематских грешака. У ту сврху, овде је изложен математички модел калибрисања ефикасности полупроводничких детектора за изворе у облику квадра. Коришћен је добро познати, проверени и поуздани принцип трансфера ефикасности при чему се ефикасност детектора рачуна на основу ефективног просторног угла Ω. У циљу провере модела, рађена су поређења са раније развијеним и темељно провереним моделима калибрације детектора за изворе са аксијалном симетријом (тачкасти, плочасти и цилиндрични). Наиме, резултати за сваки квадар који је испитиван схватани су (и проверавани) као интерполација између уписаног и описаног цилиндра исте висине, за које се ефикасности могу поуздано одредити нумеричким прорачунима (програм ANGLE). Ради целовитости увида, истовремено су рачунати и "еквиволуминозни" цилиндри. Позиционирање извора урађено је како на оси, тако и ван осе детектора (осни померај), што одговара реалним условима. Узимани су у обзир извори веома различитих димензија и пропорција, при чему су гранични случајеви представљали плочасте и тачкасте изворе. Сва рачунања рађена су у опсегу гама енергија 50-3000 keV. Резултати су логични и конзистентни, без одступања која би указивала на систематске грешке или софтверске багове, чиме убедљиво потврђују заснованост и поузданост примењеног математичког модела. Модел ће бити укључен у софтвер као нова функционалност, чиме ће бити стављен на располагање гама-спектрометријској заједници.

Кључне речи: гама-спектрометрија, ефикасност детекције, калибрација детектора, извор у облику квадра, математички модел, нумеричка провера, применљивост